https://doi.org/10.15407/ujpe69.11.767

CH. ROYON on behalf of the D0 and TOTEM Collaborations

Department of Physics and Astronomy, The University of Kansas
(Lawrence, KS 66045, USA; e-mail: christophe.royon@ku.edu)

THE DISCOVERY OF THE ODDERON BY THE D0 AND TOTEM COLLABORATIONS [1]

After a brief introduction of the odderon, we will describe its experimental discovery by the D0 and TOTEM collaborations by comparing pp and $p\bar{p}$ elastic scattering data and by combining it with the ρ and total cross section measurements by the TOTEM collaboration.

Keywords: high energy, elastic interactions, pomeron, odderon, spectrometer.

In this report, we describe the discovery of the odderon by the D0 and TOTEM collaborations [1].

1. Strategy to Observe the Odderon

In order to observe potentially the odderon [2–9], one of the best methods is to study elastic interactions, $pp \to pp$ or $p\bar{p} \to p\bar{p}$ in pp and $p\bar{p}$ interactions. These are very clean events, where nothing is produced in addition to the two intact protons/antiprotons. In order to measure these events, it is needed to detect the intact protons after interaction in dedicated detectors installed in roman pots. We use the LHC or Tevatron magnets as spectrometers. The protons are scattered at small angles, since they lost part of their energies with respect to the beam energy and deviate from the beam thanks to the magnetic field of the LHC or Tevatron magnets on the beam line.

The fact that both protons are intact after the collision can be explained by the exchange of a colorless object, which can either be a multiple number of exchanged gluons (2, 3, 4, ...) or photons between the two protons. Pomeron and Odderon correspond to positive and negative C parity. In terms of QCD, the Pomeron is made of an even number of gluons which leads to a $+1$ parity, whereas the odderon is made of an odd number of gluons corresponding to a -1 parity. The scattering amplitudes for pp and $p\bar{p}$ interactions can be written as:

$$A_{pp} = \text{Even} + \text{Odd},$$
$$A_{p\bar{p}} = \text{Even} - \text{Odd}.$$

It is clear that observing a difference between pp and $p\bar{p}$ interactions would be a clear way to observe the odderon.

The strategy to look for the odderon is thus to measure the elastic cross sections for pp and $p\bar{p}$ as a function of $|t|$, the quadri-momentum transferred square at the proton vertex measured by tracking the protons, at different center-of-mass energies and to look for potential differences. The cross section decreases as a function of $|t|$ as a power of $|t|$ at very low $|t|$ (Coulomb or QED region), then exponentially (nuclear region), and again as a power of $|t|$ in the QCD perturbative region.

Before the LHC, some differences between pp and $p\bar{p}$ elastic cross sections were already observed at ISR

Citation: Royon Ch. on behalf of the D0 and TOTEM Collaborations. The discovery of the odderon by the D0 and TOTEM collaborations. *Ukr. J. Phys.* **69**, No. 11, 767 (2024). https://doi.org/10.15407/ujpe69.11.767.

[1] This work is based on the results presented at the 2024 "New Trends in High-Energy and Low-x Physics" Conference.

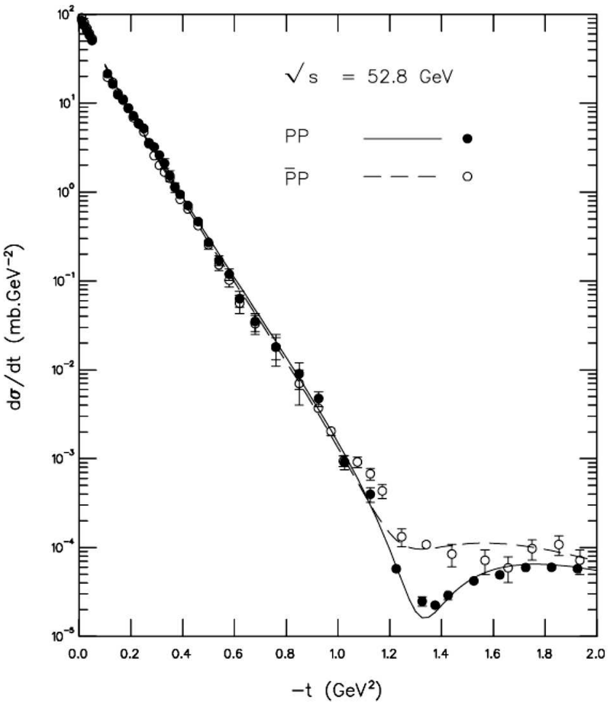

Fig. 1. Measurement of the elastic pp and $p\bar{p}$ cross sections at ISR energies

energies [10–14] as shown in Fig. 1. This was not understood as an evidence for the odderon, since, at low energies, the situation is quite complicated and elastic scattering at ISR energies can be due to the exchanges of additional particles with respect to pomeron or odderon such as ρ, ω, ϕ mesons or reggeons... The difference between pp and $p\bar{p}$ elastic cross section at ISR energies could thus be due to ω exchanges. However, at TeV energies, the cross section for meson or reggeon exchanges is negligible with respect to pomeron or odderon exchanges and differences between pp and $p\bar{p}$ elastic cross sections can be clearly seen as evidence for the odderon.

2. *pp* and *p̄p* Elastic Cross Sections at High Energies

The D0 collaboration at the Tevatron measured the elastic $p\bar{p}$ cross sections with intact p and $\bar{p}$ detected in the Forward Proton Detector [15] with 31 nb^{-1} [16] at 1.96 TeV for $0.26 < |t| < 1.2$ GeV^2, as shown in Fig. 2, *a*. The TOTEM collaboration measured the elastic pp $d\sigma/dt$ cross sections by tagging both intact protons in the TOTEM roman pots [17] at 2.76, 7, 8 and 13 TeV [18–21] as shown in Fig. 2, *b*. All TOTEM $d\sigma/dt$ pp measurements show the same features, namely, the presence of a dip and a bump in data, whereas D0 data do not show any dip or bump. As illustrated in Fig. 3, *a*, this leads to the definition of eight reference points that are characteristic of the behavior of the pp elastic $d\sigma/dt$ as a function of $|t|$, namely, the dip, the bump, bump-b, mid-1, mid-2, dip-b, bump + 5, bump + 10. This is somewhat arbitrary, but well represents the structure of pp elastic $d\sigma/dt$ at all values of $\sqrt{s}$.

The first observable that we measured is the cross section ratios between the values at the bump and at the dip as a function of the center-of-mass energy as shown in Fig. 3, *b*. The bump over dip ratio is measured for pp interactions at ISR [10–14], and LHC energies, and it decreases as a function of $\sqrt{s}$ up to $\sim$100 GeV and is flat above that energy. D0 and lower energy $p\bar{p}$ data show a ratio of 1.00 given the fact that no bump/dip is observed in $p\bar{p}$ data within uncertainties. It leads to a more than 3σ difference between extrapolated elastic TOTEM pp data and $p\bar{p}$ elastic measurement from D0 (assuming a flat behavior above $\sqrt{s} = 100$ GeV).

The difficulty to compare pp and $p\bar{p}$ elastic cross sections is that the measurements were performed at different $\sqrt{s}$ which does not allow a direct comparison. The TOTEM measurements are at 2.76, 7, 8, and 13 TeV while the D0 measurement is at 1.96 TeV. Unfortunately, it is not easy to run the LHC at about 2 TeV and there would be no acceptance in the dip/bump region, where we perform the comparison, between pp and $p\bar{p}$ elastic data. This is why we need to extrapolate the TOTEM data (or the $|t|$ and $d\sigma/dt$ values for all characteristic points) measured at 2.76, 7, 8, and 13 TeV down to the Tevatron energy of 1.96 TeV. It is worth noticing that the TOTEM measurement at 2.76 TeV is crucial for this extrapolation since the range of extrapolation between 2.76 and 1.96 TeV is not that large.

3. Extrapolating TOTEM Data at Tevatron Energies

The idea are then to determine how the values of $|t|$ and $d\sigma/dt$ of each characteristic point vary as a function of $\sqrt{s}$ in order to predict their values at 1.96 TeV. In order to avoid model-dependent fits, we use data points directly closest to those characteristic points. Data bins are also merged in case there

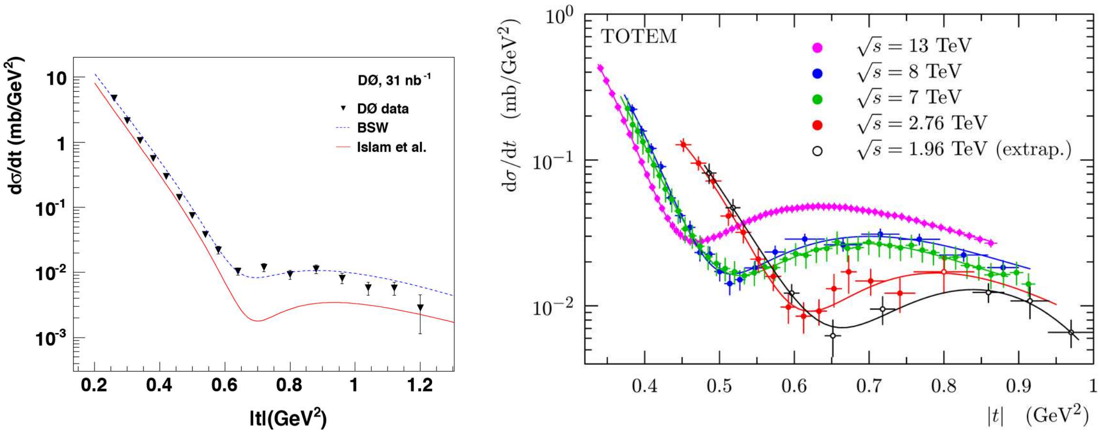

a *b*

Fig. 2. Measurement of the elastic differential cross section for $p\bar{p}$ interactions by the D0 experiment at the Tevatron (a). Same measurement for pp interactions at 2.76, 7, 8 and 13 TeV center-of-mass energies by the TOTEM Collaboration at the LHC (b)

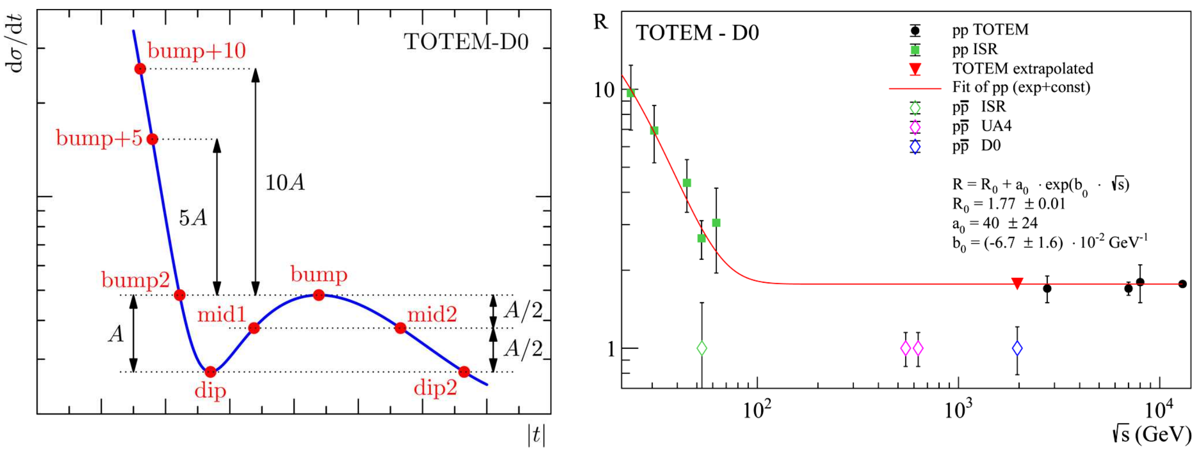

a *b*

Fig. 3. Reference points defining the shape of the pp elastic cross sections (a). Measurement of the cross section ratios between the values at the bump and at the dip as a function of the center-of-mass energy (b). We note that there is no longer any $\sqrt{s}$ dependence at TeV energies

are two adjacent dip or bump points of about equal value. This gives a distribution of t and $d\sigma/dt$ values as a function of $\sqrt{s}$ for all characteristic points as shown in Fig. 4. We can extrapolate the values of these characteristic points in $|t|$ and $d\sigma/dt$ down to the Tevatron energies using

$$|t| = a \log(\sqrt{s}[\text{TeV}]) + b,$$
$$\frac{d\sigma}{dt} = c\sqrt{s}\ [\text{TeV}] + d.$$

Alternate functional forms lead to similar results well within uncertainties. It is worth noting that it is not obvious that the same form of distribution can be used to describe the $\sqrt{s}$ evolution of all characteristic points. This shows that all curves showing the $|t|$ dependence of $d\sigma/dt$ are parallel between each other. In other words, there is a new kind of scaling appearing at high energies in LHC data [22].

4. Scaling of Elastic *pp* Data at High Energies

If one introduces the variable $t^* = (s/|t|)^A \times |t|$, inspired by the geometric scaling in terms of saturation

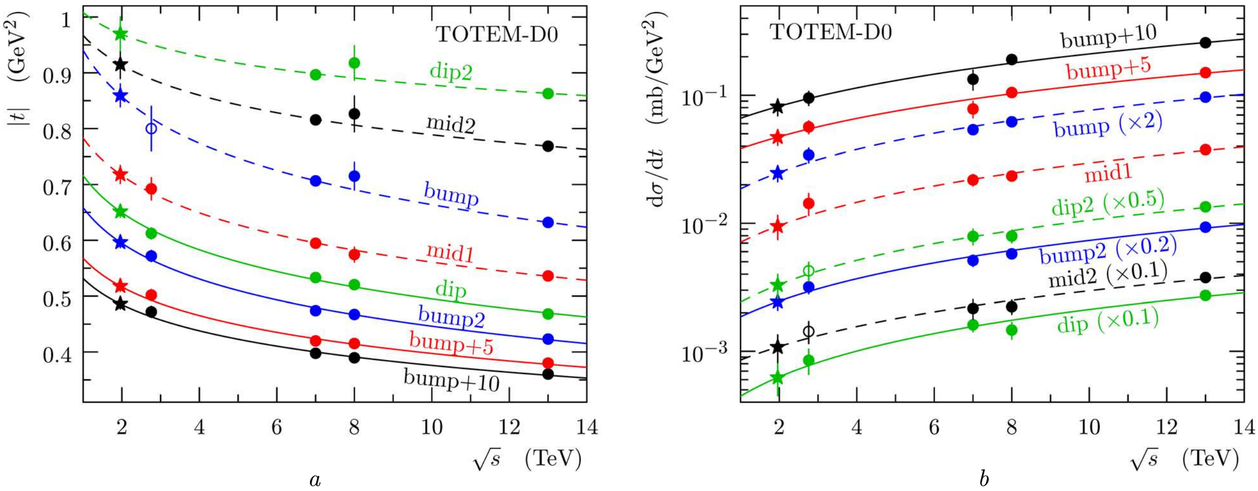

Fig. 4. Evolution of the $|t|$ and $d\sigma/dt$ values of the different characteristic points as a function of $\sqrt{s}$ and extrapolation down to the Tevatron center-of-mass energy

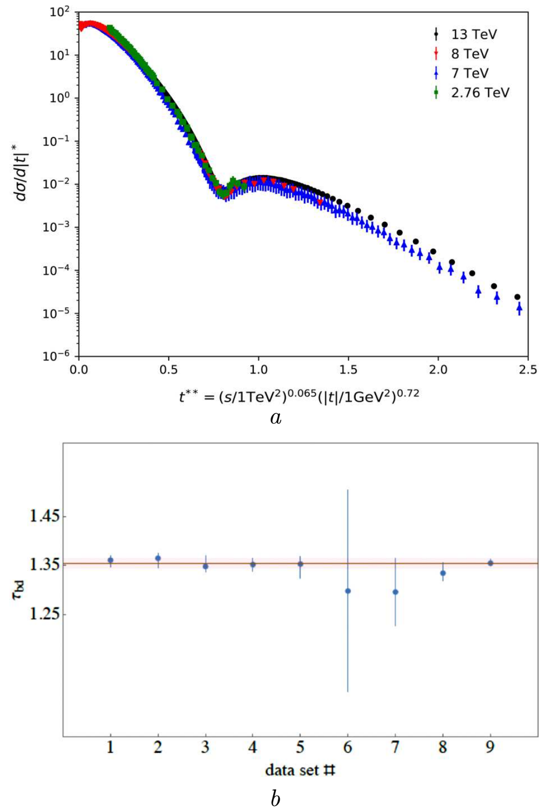

Fig. 5. Scaling shown by TOTEM *pp* elastic $d\sigma/dt^*$ cross section as a function of t^{**} ($t^{**} = t^*/s^{0.215}$ and $t^* = (s/|t|)^{0.28} \times \times |t|$) ($a$). Position ratio in $|t|$ between the bump and the dip showing it is also constant between ISR and LHC energies (b). The different numbers in abscissa correspond to ISR (1 to 5) and LHC TOTEM (6 to 9) data

models, and $t^{**} = t^*/s^B$, A and B being parameters to be fitted to data, we obtain that $d\sigma/dt^*$ shows scaling as a function of t^{**} as shown in Fig. 5, *a*. A and B are correlated and a full valley of parameters leading to similar scalings exists with the relation ($B = A - 0.065$) leading to one single parameter fit, and we obtain $A = 0.28$ [22]. Scaling could be interpreted as having a large density of gluons inside colorless gluonic compounds (responsible for diffraction) that reach the black disc limit at small impact parameter b. At higher b, the density of gluons is smaller and in principle describable by the BFKL dynamics. In another study, we also showed that the position ratio in $|t|$ between the bump and the dip is also constant between ISR and LHC energies as shown in Fig. 5, *b*, in addition to the fact that the bump over dip cross section $d\sigma/dt$ ratio is constant at high energies (see Fig. 3, *b*). This leads to an additional scaling present at high energies in the elastic scattering [23], replacing $|t| \to \tau = W^\beta |t|$ with $\beta = 0.1686$ and $\frac{d\sigma_{el}}{dt}(\tau) \to W^{-\alpha}\frac{d\sigma_{el}}{dt}(\tau)$ with $\alpha \sim 0.66$.

5. Evidence for the Odderon by Comparing *pp* and $p\bar{p}$ Elastic Data

The last step to compare D0 measurements and extrapolated TOTEM data is to predict the *pp* elastic cross section at the same t values as measured by D0 in order to make a direct comparison. We fit the reference points extrapolated to 1.96 TeV from TOTEM measurements using a double exponential fit ($\chi^2 = 0.63$ per dof)

$$h(t) = a_1 e^{-b_1|t|^2 - c_1|t|} + d_1 e^{-f_1|t|^3 - g_1|t|^2 - h_1|t|}.$$

The differences in normalization are taken into account by adjusting TOTEM and D0 data sets to have the same cross sections at the optical point $d\sigma/dt(t = 0)$. We first predict the pp total cross section from extrapolated fit to TOTEM data ($\chi^2 = 0.27$), $\sigma_{\text{tot}} = 82.7 \pm 3.1$ mb at 1.96 TeV as shown in Fig. 6. We then adjust the 1.96 TeV $d\sigma/dt(t = 0)$ from the extrapolated TOTEM data to the D0 measurement using

$$\sigma^2_{\text{tot}} = \frac{16\pi(\hbar c)^2}{1+\rho^2}\left(\frac{d\sigma}{dt}\right)_{t=0}.$$

Assuming $\rho = 0.145$, the ratio of the imaginary and the real part of the elastic amplitude, as taken from the COMPETE parametrization [25], leads to a TOTEM $d\sigma/dt(t = 0)$ at the OP of 357.1 ± 26.4 mb/GeV^2 (the exact value of ρ being of the order of 0.1 does not change much the value of σ_{tot} since it appears as ρ^2 in the formula). D0 measured the optical point of $d\sigma/dt$ at small t to be 341 ± 48 mb/GeV^2 (which is compatible with the TOTEM extrapolated measurement within uncertainties), and we rescale the TOTEM data by 0.954 ± 0.071. It is clear that we do not claim that we performed a measurement of $d\sigma/dt$ at the OP at $t = 0$ (it would require additional measurements closer to $t = 0$), but we use the two extrapolations simply in order to obtain a common and somewhat arbitrary normalization point.

The reference points at 1.96 TeV (extrapolated from the TOTEM data) are compared with the D0 measurement in Fig. 7 [1], and the χ^2 test with six degrees of freedom yields the p-value of 0.00061, corresponding to a significance of 3.4σ, leading to the evidence of the odderon by comparing pp and $p\bar{p}$ elastic data from the TOTEM and D0 experiments.

6. Combination with the ρ Measurement and Conclusion

In addition, the TOTEM collaboration measured elastic scattering at very low t in the Coulomb-Nuclear interference (CNI) region

$$\frac{d\sigma}{dt} \sim |A^C + A^N(1 - \alpha G(t))|^2.$$

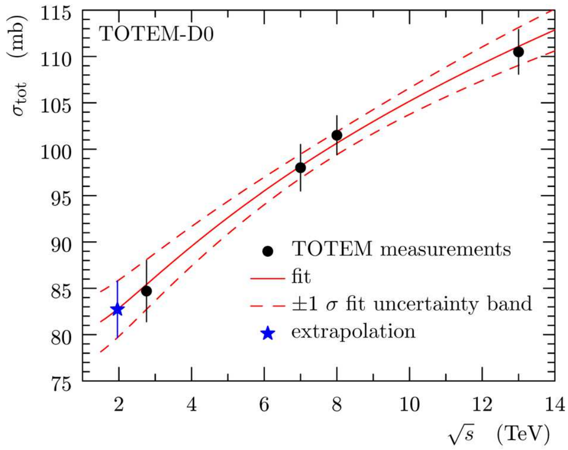

Fig. 6. Total cross section measured by the TOTEM collaboration as a function of $\sqrt{s}$ extrapolated down to the Tevatron center-of-mass energy

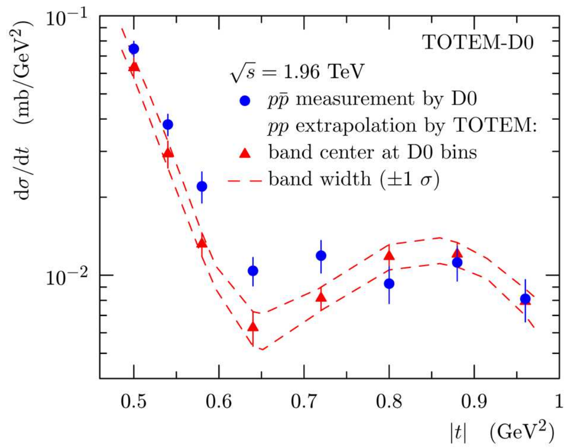

Fig. 7. Comparison between the D0 elastic $p\bar{p}$ cross section measurement at the Tevatron and the pp cross section measured by the TOTEM Collaboration at 2.76, 7, 8 and 13 TeV and extrapolated down to the Tevatron center-of-mass energy showing the evidence for the odderon

The differential cross section is sensitive to the phase of the nuclear amplitude and, in the CNI region, both the modulus and the phase of the nuclear amplitude can be used to determine

$$\rho = \frac{\text{Re}(A^N(0))}{\text{Im}(A^N(0))},$$

where the modulus is constrained by the measurement in the hadronic region and the phase by the t dependence. ρ is the ratio of the real to imaginary part of the elastic amplitude at $t = 0$, and, using low

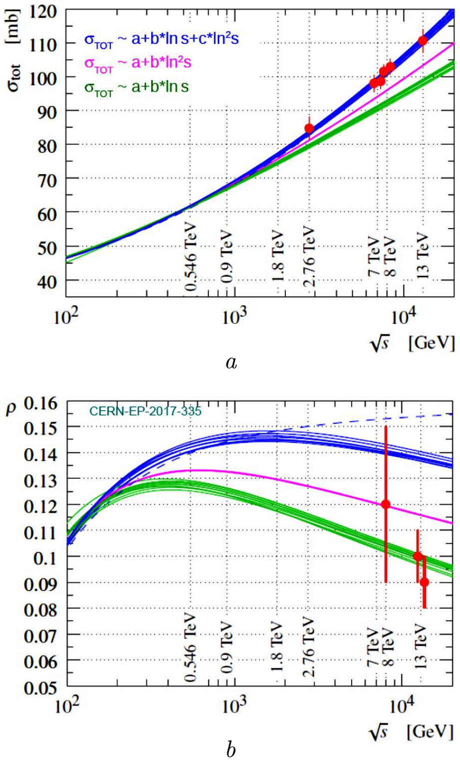

Fig. 8. Measurement of the total cross section (a) and the ρ parameter (b) as a function of $\sqrt{s}$ showing the tension between both measurement that can be explained by the effect of the odderon

$|t|$ data in the CNI region, the TOTEM Collaboration measured ρ at 13 TeV to be 0.09 ± 0.01 [24]. As shown in Fig. 8 the combination of the measured ρ and σ_{tot} values are not compatible with any set of models without odderon exchange (COMPETE predictions [25–27] are shown as an example). This result can be explained by the exchange of the Odderon in addition to the Pomeron.

Is is then possible to combine the independent evidence of the odderon found by the TOTEM Collaboration using ρ and total cross section measurements at low t with the previous evidence from the comparison between pp and $p\bar{p}$ elastic cross sections since they originate from a completely different kinematical domain. For the models included in COMPETE, the TOTEM ρ measurement at 13 TeV provided a 3.4 to 4.6σ significance, to be combined with the D0/TOTEM result. The combined significance ranges from 5.3 to 5.7σ depending on the model. It is worth noting that the D0 and TOTEM collaborations are now finalizing a detailed publication improving the present analysis shown in this report and the final significance improves by a few 0.1 digits.

It is also worth mentioning that similar roman pots detectors are now used to study $\gamma\gamma$ physics at the LHC that leads to the best sensitivities to quartic anomalous couplings and the production of axion-like particle particles, benefitting from the fact that all particles in the final state (the two intact protons and the $\gamma\gamma$, WW, ZZ, γZ, $t\bar{t}$ productions) are measured in these very clean events [28–41].

1. V.M. Abazov *et al.* Odderon exchange from elastic scattering differences between pp and $p\bar{p}$ data at 1.96 TeV and from pp forward scattering measurements. *Phys. Rev. Lett.* **127** (6), 062003 (2021).
2. L. Lukaszuk, B. Nicolescu. Possible interpretation of pp rising total cross sections. *Lett. Nuovo Cim.* **8**, 405 (1973).
3. E. Martynov, B. Nicolescu. Odderon effects in the differential cross-sections at Tevatron and LHC energies. *Eur. Phys. J. C* **79** (6), 461 (2019).
4. F. Low. Model of the bare pomeron. *Phys. Rev. D* **12**, 163 (1975).
5. S. Nussinov. Colored-quark version of some hadronic puzzles. Phys. Rev. Lett. **34**, 1286 (1975).
6. P. Gauron, L. Lukaszuk, B. Nicolescu. Consistency of the maximal odderon approach with the QFT constraints. *Phys. Lett. B* **294**, 298 (1992).
7. A. Bouquet, B. Diu, E. Leader, B. Nicolescu. A possible incompatibility between the and total cross-sections and the Regge-pole modeltotal cross-sections and the Regge-pole model. *Nuovo Cim. A* **29**, 30 (1975).
8. D. Joynson, E. Leader, B. Nicolescu, C. Lopez. Non-Regge and hyper-Regge effects in pion-nucleon charge exchange scattering at high energies. *Nuovo Cim. A* **30**, 345 (1975).
9. A.D. Donnachie, P.V. Landshoff. Multi-gluon exchange in pp elastic scattering. *Phys. Lett. B* **123** (5), 345 (1983).
10. A. Breakstone *et al.* Measurement of $\bar{p}p$ and pp elastic scattering in the dip region at $\sqrt{s} = 53$ GeV. *Phys. Rev. Lett.* **54**, 2180 (1985).
11. S. Erhan *et al.* Comparison of pp and pp elastic scattering with $0.6 < t < 2.1$ GeV^2 at the CERN-ISR. *Phys. Lett. B* **152**, 131 (1985).
12. UA4 Collaboration, D. Bernard, M. Bozzo, P.L. Braccini *et al.* Large-t elastic scattering at the CERN SPS collider at $s = 630$ GeV. *Phys. Lett. B* **171**, 142 (1986).
13. UA4 Coll., M. Bozzo, P.L. Braccini, F. Carbonara *et al.* Elastic scattering at the CERN SPS collider up to a four-momentum transfer of 1.55 GeV^2. *Phys. Lett. B* **155**, 197 (1985).
14. E. Nagy, R.S. Orr, W. Schmidt-Parzefall *et al.* Measurements of elastic proton-proton scattering at large momentum transfer at the CERN intersecting storage rings. *Nucl. Phys. B* **150**, 221 (1979).

15. V.M. Abazov *et al.* D0 Collaboration. The upgraded D0 detector. *Nucl. Instrum. Methods A* **565** 463 (2006).
16. V.M. Abazov *et al.* (The D0 Collaboration). Measurement of the differential cross section $d\sigma/dt$ in elastic $p\bar{p}$ scattering at $\sqrt{s} = 1.96$ TeV. *Phys. Rev. D* **86**, 012009 (2012).
17. G. Antchev *et al.* (TOTEM Collaboration). Performance of the TOTEM detectors at the LHC. *Int. J. Mod. Phys. A* **28**, 1330046 (2013).
18. G. Antchev *et al.* TOTEM Collaboration. Elastic differential cross-section $d\sigma/dt$ at $\sqrt{s} = 2.76$ TeV and implications on the existence of a colourless C-odd three-gluon compound state. *Eur. Phys. J. C* **80** (2), 91 (2020).
19. G. Antchev *et al.* TOTEM Collaboration. Proton-proton elastic scattering at the LHC energy os $\sqrt{s} = 7$ TeV. *Europhys. Lett.* **95**, 41004 (2011).
20. G. Antchev *et al.* Evidence for non-exponential elastic protonпїЅproton differential cross-section at low $|t|$ and $s = 8$ TeV by TOTEM. TOTEM Collaboration. *Nucl. Phys. B* **899**, 527 (2015).
21. G. Antchev *et al.* Elastic differential cross-section measurement at $\sqrt{s} = 13$ TeV by TOTEM. (TOTEM Collaboration). *Eur. Phys. J. C* **79** (10), 861 (2019).
22. C. Baldenegro, C. Royon, A. Sasto. Scaling properties of elastic proton-proton scattering at LHC energies. *Phys. Lett. B* **830** (2022) 137141.
23. C. Baldenegro, M. Praszalowicz, C. Royon, A. Stasto. Diffraction and saturation at the LHC. *Phys. Lett. B* **856**, 13896 (2024).
24. G. Antchev *et al.* First determination of the parameter at TeV: probing the existence of a colourless C-odd three-gluon compound state: TOTEM Collaboration. *Eur. Phys. J. C* **79** (9), 785 (2019).
25. J. R. Cudell, V. V. Ezhela, P. Gauron *et al.* COMPETE Coll. Benchmarks for the forward observables at RHIC, the Tevatron-Run II, and the LHC. *Phys. Rev. Lett.* **89**, 201801 (2002).
26. V.A. Khoze, A.D. Martin, M.G. Ryskin. Elastic and diffractive scattering at the LHC. *Phys. Lett. B* **784**, 192 (2018).
27. M.M. Block, L. Durand, P. Ha, F. Halzen. Comprehensive fits to high energy data for σ, ρ, and B, and the asymptotic black-disk limit. *Phys. Rev. D* **92**, 114021 (2015).
28. E. Chapon, C. Royon, O. Kepka. Anomalous quartic $WW\gamma\gamma$, $ZZ\gamma\gamma$, and trilinear $WW\gamma$ couplings in two-photon processes at high luminosity at the LHC. *Phys. Rev. D* **81**, 074003 (2010).
29. O. Kepka, C. Royon. Anomalous $WW\gamma$ coupling in photon-induced processes using forward detectors at the CERN LHC. *Phys. Rev. D* **78**, 073005 (2008).
30. S. Fichet, G. von Gersdorff, B. Lenzi, C. Royon, M. Saimpert. Light-by-light scattering with intact protons at the LHC: from standard model to new physics. *JHEP* **2**, 165 (2015).
31. S. Fichet, G. von Gersdorff, O. Kepka, B. Lenzi, C. Royon. Probing new physics in diphoton production with proton tagging at the Large Hadron Collider. *Phys. Rev. D* **89**, 114004 (2014).
32. C. Baldenegro, G. Biagi, G. Legras, C. Royon. Central exclusive production of W boson pairs in pp collisions at the LHC in hadronic and semi-leptonic final states. *JHEP* **12**, 165 (2020).
33. C. Baldenegro, S. Fichet, G. von Gersdorff, C. Royon. Central exclusive production of W boson pairs in pp collisions at the LHC in hadronic and semi-leptonic final states. *JHEP* **6**, 142 (2017).
34. C. Baldenegro, A. Bellora, S. Fichet, G. von Gersdorff, M. Pitt, C. Royon. Searching for anomalous top quark interactions with proton tagging and timing detectors at the LHC. *JHEP* **8**, 021 (2022).
35. A. Tumasyan, W. Adam, J.W. Andrejkovic *et al.* CMS and TOTEM Coll. Search for high-mass exclusive $\gamma\gamma \to WW$ and $\gamma\gamma \to ZZ$ production in proton-proton collisions at $\sqrt{s} = 13$ TeV. *JHEP* **7**, 229 (2023).
36. A. Tumasyan, W. Adam, J.W. Andrejkovic *et al.* (CMS and TOTEM Collaboration). Search for central exclusive production of top quark pairs in proton-proton collisions at $\sqrt{s} = 13$ TeV with tagged protons. *JHEP* **6**, 187 (2024).
37. A. Tumasyan, W. Adam, J.W. Andrejkovic *et al.* (CMS and TOTEM Collaboration). Search for high-mass exclusive $\gamma\gamma \to WW$ and $\gamma\gamma \to ZZ$ production in proton-proton collisions at $\sqrt{s} = 13$ TeV JHEP **7**, 229 (2023).
38. A. Tumasyan *et al.* (CMS and TOTEM Collaboration). First search for exclusive diphoton production at high mass with tagged protons in proton-proton collisions at $\sqrt{s} = 13$ TeV. *Phys. Rev. Lett.* **129** (1), 011801 (2022).
39. A. Tumasyan, W. Adam, J.W. Andrejkovic *et al.* (CMS and TOTEM Collaboration). Search for high-mass exclusive diphoton production with tagged protons in proton-proton collisions at $\sqrt{s} = 13$ TeV. *Phys. Rev. D* **110**, 012010 (2024).
40. C. Baldenegro, S. Fichet, G. von Gersdorff, C. Royon. Searching for axion-like particles with proton tagging at the LHC. *JHEP* **6**, 131 (2018).
41. C. Baldenegro, S. Hassani, C. Royon, L. Schoeffel. Extending the constraint for axion-like particles as resonances at the LHC and laser beam experiments. *Phys. Lett. B* **795**, 339 (2019).

Received 07.10.24

К. Руайон від імені колаборацій D0 і TOTEM

ВІДКРИТТЯ ОДЕРОНУ КОЛАБОРАЦІЯМИ D0 І TOTEM

Після короткого ознайомлення з одероном, ми опишемо його експериментальне відкриття колабораціями D0 і TOTEM, порівнюючи дані для пружного розсіяння pp і $p\bar{p}$ та поєднуючи їх із вимірюваннями перерізу для ρ і повного перерізу, проведеними колаборацією TOTEM.

Ключові слова: високі енергії, пружні взаємодії, померон, одерон, спектрометр.